Available online at www.sciencedirect.com
SCIENCE DIRECT®
Composite Structures 67 (2005) 299–306
COMPOSITE STRUCTURES
www.elsevier.com/locate/compstruct

An investigation on the effect of a small mass impact on sandwich composite plates

J. Christopherson *, M. Mahinfalah *, G. Nakhaie Jazar, M. Rastgaar Aagaah

Department of Mechanical Engineering and Applied Mechanics, North Dakota State University, Dolve 105, P.O. Box 5285, Fargo, ND 58105, USA

Available online 25 August 2004

Abstract

This paper investigates the high strain rate response of polymer matrix sandwich composites utilizing foam-filled honeycomb cores by means of a small mass impact. The reinforcement fiber chosen for use in this paper is a simple weave carbon fiber. This paper also investigates the effects of utilizing different laminate configurations in conjunction with investigation of the effectiveness of such laminate during impact loading. In an effort to ascertain more information about the impact situation, compression after impact tests are performed to determine the extent of the damage by observing the degradation of strength associated with the impact event.

Keywords: Sandwich composite; Honeycomb structures; Small mass impacts; Carbon fiber

1. Introduction

This paper investigates the high strain rate (HSR) response of polymer matrix composites undergoing small mass impact. High velocity, small mass impacts may be imparted onto the composite structure courtesy of runway/roadway debris and hailstones to name a few. This type of impact may cause excessive local damage to the composite. Impacts of such nature also exist for only a short amount of time inducing a HSR response, a response governed by wave propagation, which are often times incorrectly labeled "high velocity impact" [1].

The HSR response of sandwich composites is investigated by comparison of impact energies, absorbed energies, and residual compressive strength after impact. The use of impact energy as a method for determining the criticality of an impact event is chosen due not only to its relevance in the study of impact situations, but in its simplicity as a possible tool for design applications. The absorbed energy is approximated in an effort to better understand the HSR behavior of sandwich composites. More specifically, the absorbed energy allows insight into the damage induced courtesy of impact situations and the influence of each individual component of the sandwich structure.

There are several mechanisms for energy absorption in sandwich composites, most notably, fiber-matrix delamination and debonding in conjunction with face-sheet to core delamination [2]. The delamination between face-sheet and core due to impact also appears to be a function of the material each respective component is made from [3]. In addition, the specific geometry of the core becomes critical in core to face-sheet bond strength. More specifically, the amount of surface area allowed for bonding between the core and face-sheet dramatically effects the stress distribution throughout the composite. Cores made from honeycomb structures typically can exhibit difficulties in bond adhesion to the face-sheet due to the lack of usable surface area for bonding. Filling the honeycomb structure with foam

* Corresponding authors. Tel.: +1 701 231 5180/799 3547; fax: +1 701 231 8913 (J. Christopherson), tel.: +1 701 231 8839; fax: +1 701 231 8913 (M. Mahinfalah).
E-mail addresses: jason.christopherson@ndsu.nodak.edu (J. Christopherson), m.mahinfalah@ndsu.nodak.edu (M. Mahinfalah).

0263-8223/$ - see front matter © 2004 Elsevier Ltd. All rights reserved.
doi:10.1016/j.compstruct.2004.07.013

can alleviate many of the bonding issues associated with honeycomb structures by providing a more favorable stress distribution via increased bond surface area [3]. In addition, by filling the structure with foam, the foam provides increased support to the honeycomb core. The core is then capable of increased impact resistance and can readily transfer higher loads to adjacent cells. The core also features increased fracture resistance in conjunction with increased moment resistance [3].

2. Literature review

Much of the literature to date focusing on HSR responses in composite materials has utilized split Hopkinson pressure bar (SHPB) [3,4]. This literature shows that the major mechanism of failure for a sandwich composite undergoing HSR loading is core failure with almost no appreciable face-sheet to core delamination. This is in contrast to low-velocity impact situations, which have received much attention lately, in which a primary mode of failure is delamination [2,5–8]. In addition, there has been some work concerning small mass impacts on sandwich composite materials. Work in this region has shown that high-velocity/low-mass impacts impart a wave-controlled response such that the load and deflection responses are out of phase and independent of the composite panels boundary conditions or size [1].

The work on small mass impact addresses the initiation of matrix cracking and delamination. Olsson attributes the initial matrix cracking due to high local contact stresses, which initiate at relatively low-loads. However, the onset of delamination is typically reserved for higher impact loads. Therefore, the peak impact force becomes a key parameter [1]. Olsson also shows that at low-velocity, the impact response is governed by the impactor/plate mass ratio as compared to the impact velocity for higher-velocity impacts [1].

The use of in-plane compressive loading to identify the criticality of the damage induced by impact is an idea that has been given some attention in recent years. The importance of such investigation is attributed to the need to identify the remaining capability of the composite to withstand static loading conditions after the composite has been exposed to an impact event [9]. In addition, the criticality of the damage induced by an impact event may be more readily determined via compressive loading. This is because while under compressive loading a delaminated face-sheet has the tendency to respond free of the remainder of the composite thereby exposing the damaged region [10].

3. Manufacturing methods

All composite panels used in this investigation were constructed using a bag molding technique such that the resulting composite panel would be of high quality and relatively defect free [11,12]. Although this procedure is rather time consuming, the quality of the composite laminate was of prime concern; therefore, the bag molding process was chosen. In addition to yielding a high quality composite laminate, the bag molding process lends itself very well to the manufacture of flat composite panels such as required for this investigation. Fig. 1 illustrates the manufacturing set-up used.

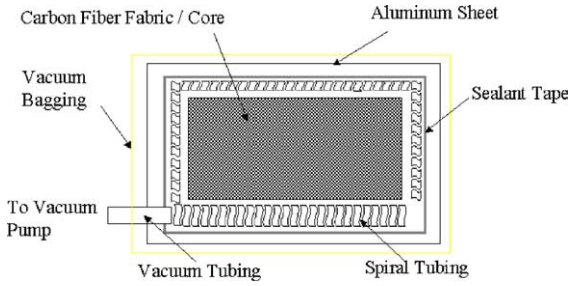

Fig. 1. Manufacturing set-up.

In this study an epoxy resin was used for the matrix material, which polymerized at room temperature. Carbon fiber was chosen as the reinforcement due to its inherently high strength and high modulus of elasticity. The carbon fiber used was a simple weave carbon cloth. However, no alteration of fiber reinforcement angle was utilized while assembling the face-sheet lamina. That is, all layers of the face-sheet utilized the same orientation.

The epoxy used for this study was purchased from Eastpointe Fiberglass Sales, Inc., with the resin part number F-82 and the hardener TP-41F. The epoxy was mixed according to the following recommended ratio by weight: 100 parts resin for 25 parts hardener. The carbon fiber utilized was 3K plain weave graphite fabric #530. In addition, the foam-filled honeycomb core was provided by General Plastics Manufacturing Company and was part number FR-FFHC-08.

The quality of the composite samples was ensured by randomly taking samples and magnifying them to obtain information regarding the fiber volume fraction of the face-sheets, the fiber volume fraction for samples tested averaged 43% as found by examination under microscope.

4. Experimental procedures

All tests were conducted by first verifying the accuracy of the chronographs with respect to calibrated values. Once this was completed, the desired test samples were loaded into the pneumatic gun shown in Fig. 2, and clamped along the outer edges of the plate from both the front and back of the composite plate. Then the tank pressure was brought to an appropriate level to achieve the desired projectile velocity. The projectile would then

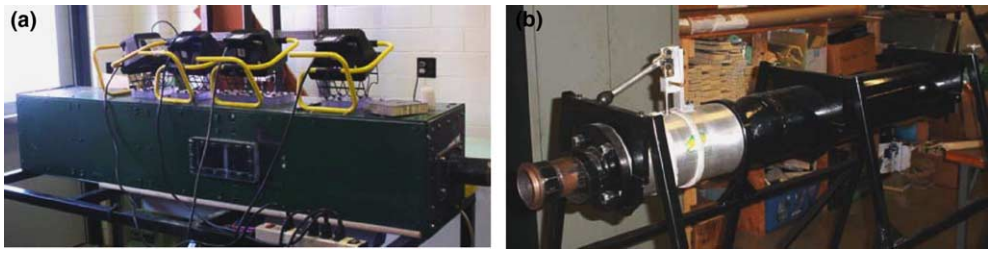

Fig. 2. (a) Pneumatic gun sample chamber. (b) Pneumatic gun firing mechanism.

be fired at the center of the sample and velocity measurements of the projectile were taken immediately before impact with the sample and directly after the projectile exited the sample. This procedure was repeated at several different tank pressures (i.e. several different impact velocities). If the projectile did not exit the sample, it became obvious that the kinetic energy has been lost to deform both the sample and the projectile along with any thermal energy released. However, for the purposes of this study, the energy lost due to projectile deformation and thermal effects were neglected due to the small values associated with such energy losses as compared to the initial kinetic energy of the projectile.

The projectile is a 12.7 mm (0.5 in.) diameter steel slug with a mass of 16 g. The velocity range utilized for this test was in the range of approximately 80–150 m/s (maximum safe velocity). The sample is 127 mm (5 in.) in width and height.

Upon completion of impact testing, the samples were subjected to in-plane compressive loading in an effort to determine the damage effects of the impact courtesy of residual compressive strength of the composite panel. In addition, the compression after impact (CAI) test was designed to highlight the presence of localized delamination caused by excessive localized lamina buckling. However, global panel buckling was prevented by the use of anti-buckling fixtures as shown in Fig. 3.

4.1. Experimental results and discussion

Velocity measurements taken from the chronographs were utilized to calculate the loss of the projectiles kinetic energy and were calculated as follows.

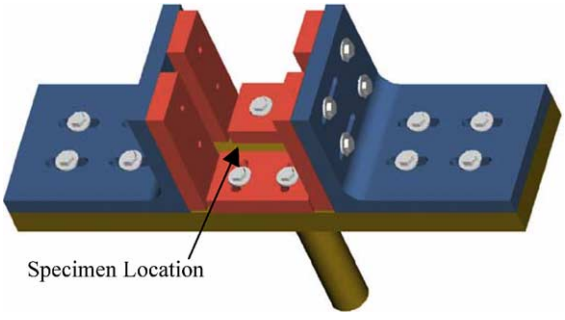

Fig. 3. Compression after impact fixture.

$$E = \frac{1}{2}m(v_i^2 - v_f^2) \tag{1}$$

where v_i is the initial velocity, v_f is the final velocity, m is the mass of the projectile and E is the kinetic energy loss of the projectile.

Eq. (1) neglects any energy dissipated by the projectile while it deforms, but the energy involved in deformation of the projectile is negligible when compared to the initial kinetic energy of the projectile. Eq. (1) also neglects any thermal energy transfer by again assuming this energy transfer to be negligible with respect to the initial kinetic energy of the projectile.

For this investigation five distinct sample types were tested. These consisted of three 25.4 mm core samples, one 15.9 mm core sample and one carbon laminate. The three 25.4 mm core samples consisted of samples containing two face-sheets, one face-sheet on the impacted side, or one face-sheet on the non-impacted side. The one face-sheet samples were utilized to determine the effectiveness of not only the core on the overall energy absorption characteristics of the sample, but also the effectiveness of the face-sheets on the energy absorption characteristics. The two face-sheet 15.9 mm samples were utilized to determine the effectiveness of the core thickness on energy absorption characteristics, and the single laminate samples provided a means by which to judge the effectiveness of the face-sheets without influence of the core.

Fig. 4 illustrates the absorbed energy of each sample type as a function of impact energy. As readily may be noticed, samples with thicker foam-filled cores and face-sheets on multiple sides provide the best resistance to impact. More specifically, these samples illustrate an increased capacity to absorb energy due to an impact event. This response tends to indicate not only the functionality of the face-sheets in an impact event, but also the improved energy absorption capabilities of the thicker core. Closer examination yields the observation that the foam-filled core provides the majority of the energy absorption capabilities due to its capability to dampen the stress wave propagation through the sample [12,13].

15.9 mm (5/8″) two face-sheet sample: Fig. 5 illustrates the HSR behavior of the sample consisting of a 15.9 mm thick core with two 4-ply face-sheets. This figure shows not only the actual data points, but also a

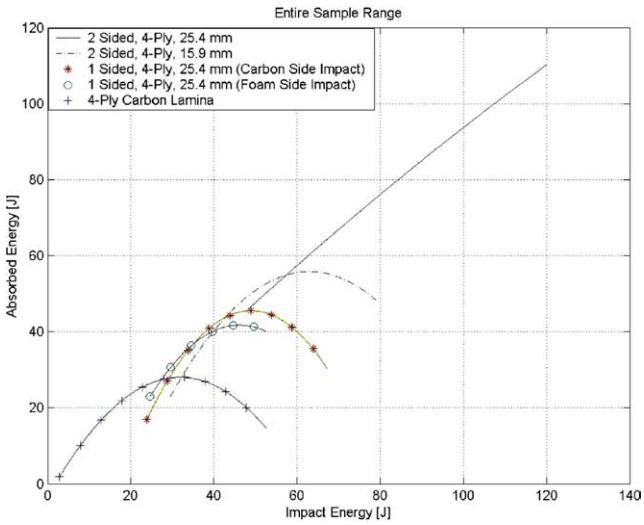

Fig. 4. Impact energy as compared to absorbed energy.

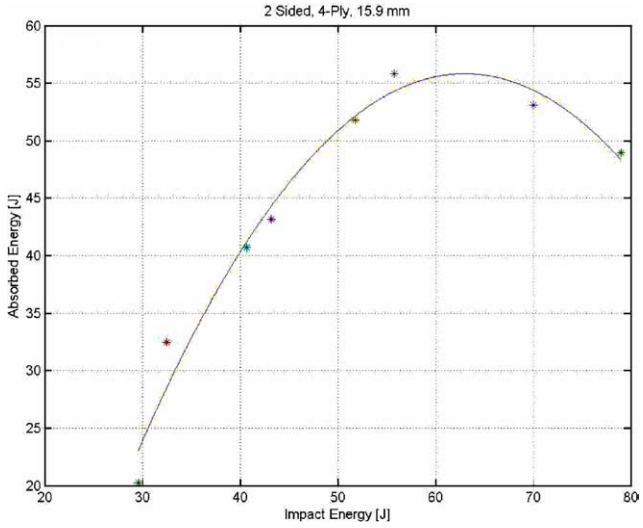

Fig. 5. Impact energy with respect to absorbed energy (15.9 mm core/2 face-sheets).

curve fitted to the data by a least squares procedure to better illustrate and understand the trend associated with increasing impact energy. This curve yields a maximum absorbed energy of 55.8 J at an impact energy of 63.1 J. In addition, any impact at an energy greater than the aforementioned critical value appears to create a dramatic increase in the amount of localized damage due to the impact event. Fig. 6 and Tables 1 and 2 illustrate that after an impact exceeding the critical energy value, the residual strength of the composite degrades in a rapid fashion thereby ensuring the presence of an increased damage area. This damage area appears to consist of both fiber and matrix failure, but also consists of an increasing interlaminar delamination area. The presence of this delamination area was verified during the compression after impact (CAI) tests by noting the first

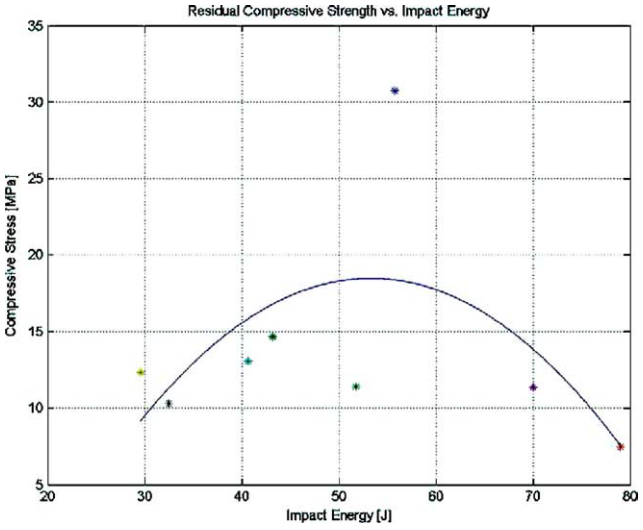

Fig. 6. Residual strength with respect to impact energy (15.9 mm core/2 face-sheets).

mode of failure in samples that had undergone excessively high energy impacts appeared to be localized buckling of the carbon laminates. The localized buckling indicates a lack of interlaminar adhesion, more specifically, the presence of interlaminar delamination.

25.4 mm (1″) two face-sheet sample: Fig. 7 illustrates the HSR behavior of the composite sample consisting of a 25.4 mm. thick foam filled honeycomb core in conjunction with two 4-ply carbon laminate face-sheets (one per side). This sample showed a maximum absorbed energy of 110.2 J at an impact energy of 120.0 J. However, the absorbed energy of 110.2 J does not appear to be a maximum absorbed energy noting the curve fit to the data is still approximately linear and therefore has not yielded a maximum value. This also can be further verified by examination of Fig. 8 and Tables 1 and 2 by noting that the residual strength has not yet begun to degrade. In addition, Fig. 8 illustrates a trend that appears common to all damaged composite samples tested. That is the increase in residual strength until the impact energy reaches the critical energy value for the particular sample. This appears to be attributed to the decreasing size of the damage area as impact velocity, hence energy, increases, assuming the critical energy value has not been exceeded. The decrease in the damage area indicates the lack of interlaminar delamination showing the only failure mechanism of the composite as localized fiber and matrix cracking. However, under compressive loading, it is the fiber and matrix cracking that acts as a stress concentration thereby causing an initiation site of failure for the composite under static load.

25.4 mm (1″) one face-sheet sample Figs. 8 and 9 illustrate the impact response of samples utilizing a 25.4 mm thick foam-filled honeycomb core in conjunction with one 4-ply face-sheet consisting. Fig. 9 illustrates the effects of impact when the sample is

Table 1
Compressive strengths obtained from CAI test results

Sample type	Maximum compressive strength after impact (curve-fit) [MPa]	Maximum compressive strength after impact (experimental) [MPa]
4-ply laminate	10.07	9.54
15.9 mm, 2-sided	18.49	30.72
25.4 mm, 2-sided	8.03	8.46
25.4 mm, 1-sided[a]	5.69	6.40
25.4 mm 1-sided[b]	7.59	10.01

[a] Carbon side impact.
[b] Foam side impact.

Table 2
Summary of HSR response values

Sample type	Maximum impact velocity [m/s]	Maximum impact energy [J]	Maximum absorbed energy [J]	Critical impact energy [J]
4-ply lamina	81.1	52.6	28.0	31.9
15.9 mm, 2-sided	99.4	79.0	55.8	63.1
25.4 mm, 2-sided	122.5	120.1	110.2	120.0
25.4 mm, 1-sided[a]	91.7	67.2	45.5	48.9
25.4 mm, 1-sided[b]	81.1	52.6	41.8	46.1

[a] Carbon side impact.
[b] Foam side impact.

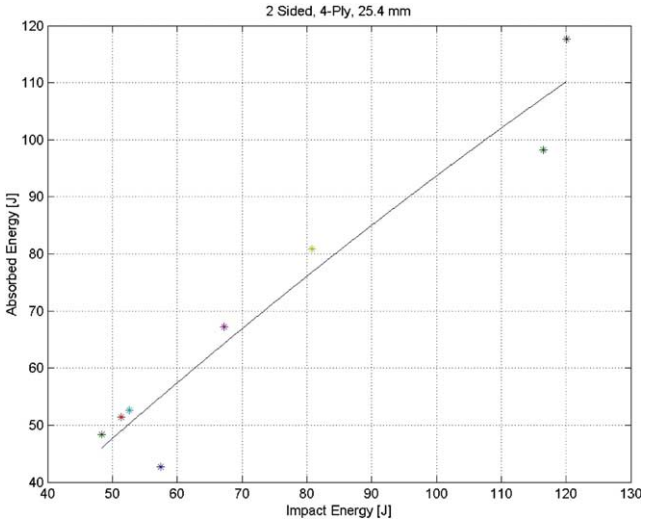

Fig. 7. Impact energy with respect to absorbed energy (25.4 mm core/2 face-sheets).

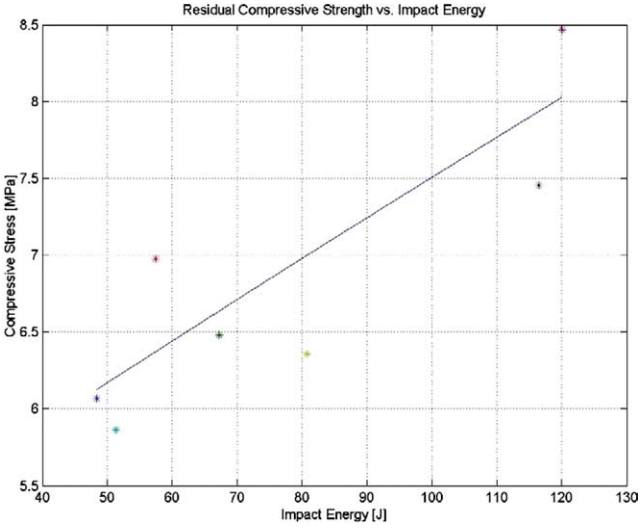

Fig. 8. Residual strength with respect to impact energy (25.4 mm core/2 face-sheets).

impacted on the face-sheet side and Fig. 10 illustrates the impact behavior of a sample impacted on the opposite side from the laminate. Each sample again exhibits a noticeable critical energy value with the laminate side impacted samples indicating a maximum absorbed energy of 45.5 J at an impact energy of 48.9 J. Where as the samples impacted from the opposite side yield a maximum absorbed energy of 41.8 J at an impact energy of 46.1 J. In addition, Fig. 11 and Tables 1 and 2 illustrate the residual strength of the samples impacted from the side opposite the face-sheet. Fig. 12 and Tables 1 and 2 illustrate the residual strength of the samples impacted on the face-sheet side.

4-ply carbon laminate: The 4-ply carbon laminate was tested in an effort to determine the response of the face-sheets and to verify the effect of the foam filled core on the impact response of the sandwich composite. Fig. 13 illustrates the impact response of the 4-ply laminate. These samples indicate the energy absorption capabilities of the laminate face-sheets. As would be expected, the energy absorption capabilities of the laminate alone do not approach that of the sandwich as a whole. This may be attributed solely to the core structure. However, the laminate does show a reasonable amount of energy absorption characteristics with a maximum absorbed

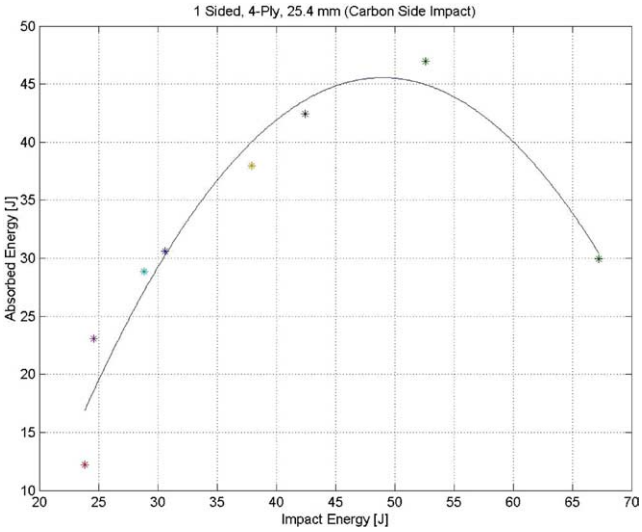

Fig. 9. Impact energy with respect to absorbed energy (25.4 mm core/1 face-sheet, carbon side).

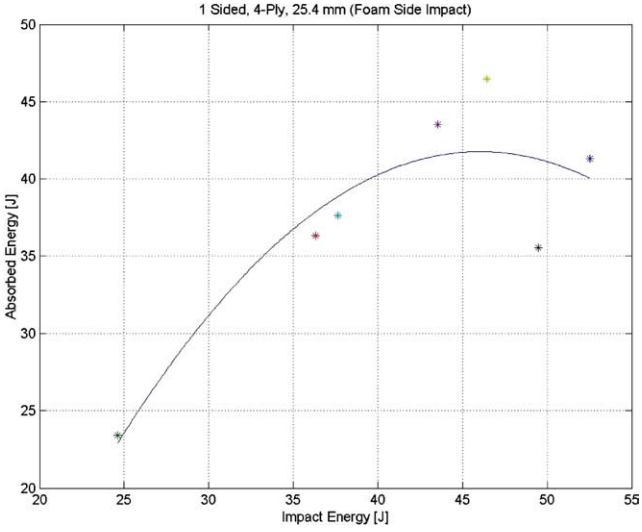

Fig. 10. Impact energy with respect to absorbed energy (25.4 mm core/1 face-sheet, foam side).

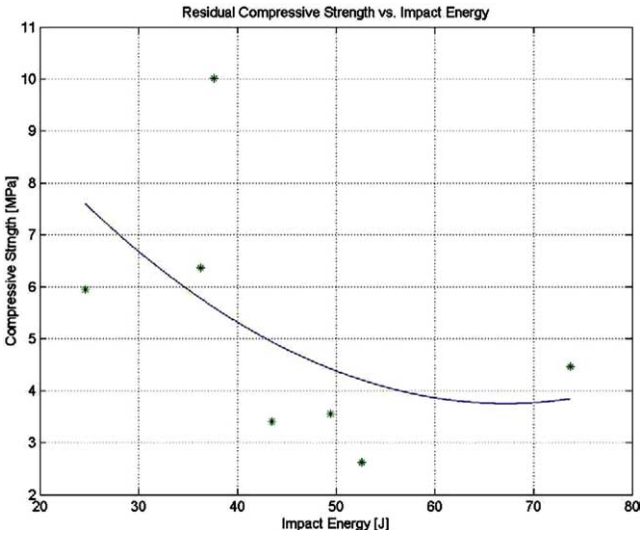

Fig. 11. Residual strength with respect to impact energy (25.4 mm core/1 face-sheet, foam side).

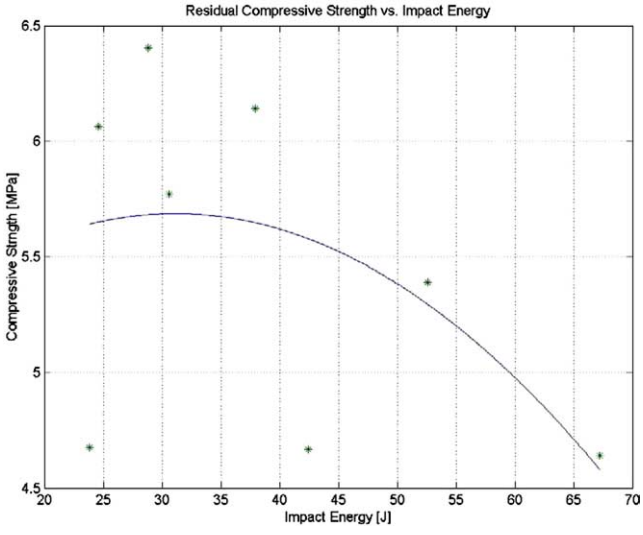

Fig. 12. Residual strength with respect to impact energy (25.4 mm core/1 face-sheet, carbon side).

energy of 28.0 J at an impact energy of 31.9 J as compared to other samples in which a foam-filled honeycomb core was utilized.

The response of the 4-ply laminate to in-plane compressive loading (Fig. 14 and Tables 1 and 2) shows similar trends to the other samples tested. The presence of a critical impact energy value may easily be obtained, and for this particular sample, the critical impact energy obtained courtesy of the curve fit to the compression data is 29.7 J.

It appears that the low-energy impacts on the 4-ply laminate did not generate any noticeable damage after a visual inspection. However, Fig. 14 illustrates these samples to have a rather low-strength. From this observation, the conclusion may be drawn that there exists some interlaminar damage that cannot be detected by visual inspection alone. The degree of strength degradation appears to be significant enough to ensure the presence of interlaminar delamination due to the impact event.

In all CAI samples, several modes of failure were noticed. Initially, the rear face-sheet would experience localized buckling indicating the presence of local delamination. After the onset of local buckling, both face-sheets would experience rapid crack propagation extending from the outermost regions of the damaged area. Finally, the sandwich would experience a core shear failure once the face-sheets were incapable of supporting additional load. These results seem to be in approximate agreement with the findings of

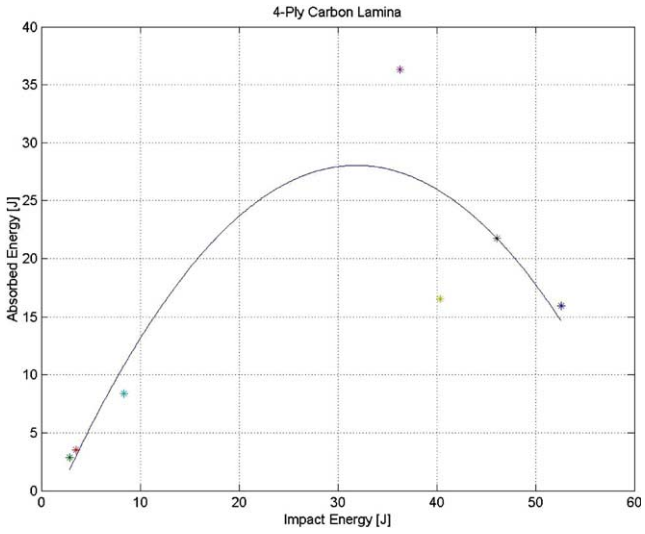

Fig. 13. Impact energy with respect to absorbed energy (4-ply carbon laminate).

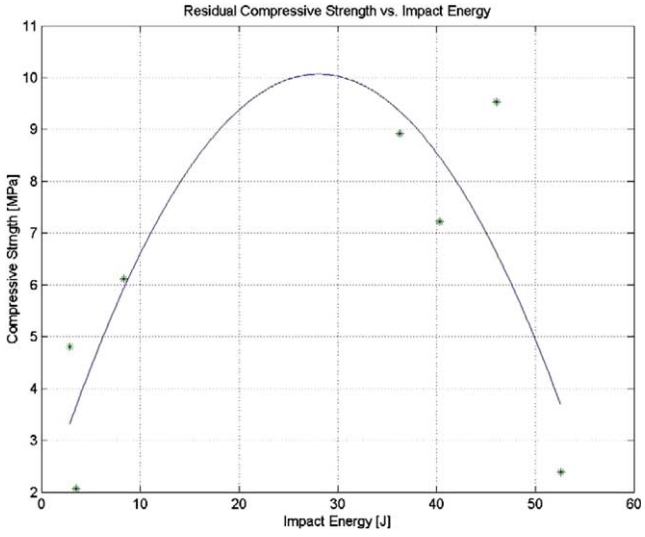

Fig. 14. Residual strength with respect to impact energy (4-ply carbon laminate).

Kwon et al. [10] for a sandwich composite containing both a hole and delamination. However, the onset of localized buckling was dependent upon the impact energy that is, it was dependent upon the amount of damage caused by the impact event. As shown in Figs. 6, 8, 11, 12 and 14, the samples impacted near their respective critical impact energies exhibited the highest strength, and from visual inspection, these samples exhibited the least amount of local buckling. Therefore, the samples impacted just below their critical energy levels had a minimized damage area.

Fig. 15 illustrates the damage induced by the impact and CAI testing. Fig. 15a. shows the non-impacted side of a 25.4 mm core, two face-sheet sample, illustrating the magnitude of the damage caused by the projectile. As can be readily seen, the damage area is much larger than the projectile diameter (noted by the hole in the core) due to not only matrix cracking but fiber failure as well. Fig. 15b. illustrates the impact side of the same composite sample. This figure shows the relative lack of damage, except for the local damage induced by the penetration of the projectile. Fig. 15c. illustrates a composite panel loaded to failure under in-plane compressive forces. Two prominent features exist. First, the local delamination initially caused by of the impact situation has been further enhanced because of the compressive loading, and second, the propagation of cracks initiating from the damage area perpendicular to the loading direction. Not visible in this figure is the shear failure of the core itself.

Fig. 16 illustrates a cross-section of the damaged area of 25.4 mm core, two face-sheet sample after experiencing an impact of 120 J and after compressive failure from the CAI testing. As may be readily seen, the damaged area is relatively local to the impacted region. Localized delamination on the non-impact side of the plate is readily apparent as is the damage induced to the core by the projectile. In addition, the impact side face-sheet cracking is readily apparent.

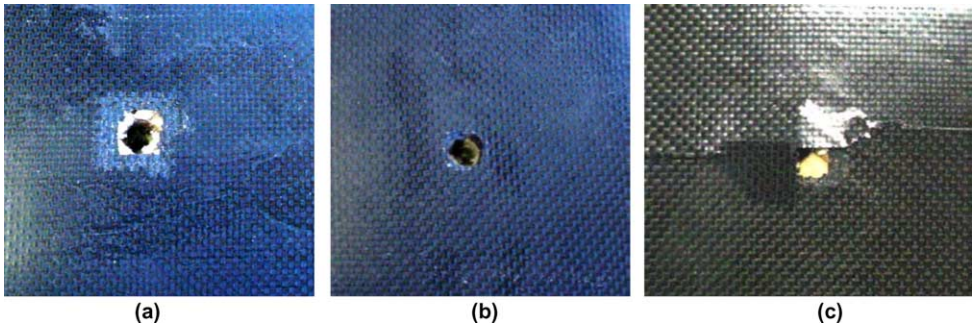

Fig. 15. Non-impacted side damage (25.4 mm core, two face-sheets/120 J impact). Impact side damage (25.4 mm core, two face-sheets/120 J impact). Compression (after impact) damaged sample (15.9 mm core, two face-sheets/43 J impact). (a) Non-impacted side damage (25.4 mm core, two face-sheets/120 J impact. (b) Impact side damage (25.4 mm core, two face-sheets/120 J impact). (c) Compression (after impact) damaged sample (15.9 mm core, two face-sheet/43 J impact).

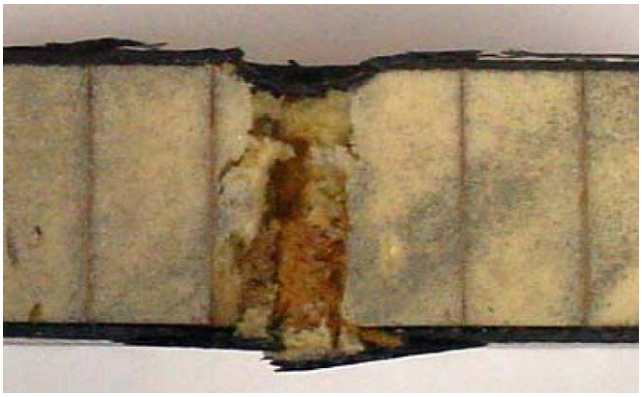

Fig. 16. 25.4 mm sample after 120 J impact and compressive failure.

5. Conclusions

By analyzing the results from both HSR and CAI testing it appears that the impact velocity, hence kinetic energy of a projectile, has a dramatic effect on the criticality of the damage induced to the composite. Once the velocity approaches a critical value, dependent upon sandwich material and geometry of the composite panel, the damage area induced by the impact situation is quite local until the impact energy approaches and exceeds the respective critical energy value for the respective panel.

CAI testing also appears to reveal that while any impact event causes degradation in the composite panel's compressive strength, the degradation becomes most severe after the impact event has exceeded the critical energy value for the particular panel type. In addition, CAI testing tends to indicate the increased presence of interlaminar cracking and delamination on samples with larger visible damage areas. This is not to say that impact events occurring below the critical energy value for the sample do not initiate interlaminar damage (as witnessed directly in the 4-ply laminate samples), but more specifically, they do not induce the amount of damage observed at higher impact energies. However, the panels impacted near their respective critical energy values tended to show the least degradation of compressive strength. At this energy level, the damage area was again quite local, and judging by the residual compressive strength of the panels, this type of impact may have generated the least interlaminar damage. There is only one sample type that showed exception to this rule, and that was the 25.4 mm core sample with one face-sheet, which was impacted on the non-laminate side. This is because the foam alone is not capable of fully absorbing the kinetic energy of the projectile; therefore, the kinetic energy of the projectile created excessive interlaminar damage in conjunction with causing damage to the bond between core and face-sheet.

Acknowledgment

The National Science Foundation, under grant 0082832, and the NASA Space Grant Fellowship Program provided funding for this research. Their support is greatly appreciated.

References

[1] Olsson R. Closed form prediction of peak load and delamination onset under small mass impact. J Compos Struct 2003;59:341–9.
[2] Torre L, Kenny JM. Impact testing and simulation of composite sandwich structures for civil transportation. J Compos Struct 2000;50:257–67.
[3] Vaidya UK, Nelson S, Sinn B, Mathew B. Processing and high strain rate impact response of multi-functional sandwich composites. J Compos Struct 2001;52:429–40.
[4] Mahfuz H, Mamun WA, Haque A, Turner S, Mohamed H, Jeelani S. An innovative technique for measuring the high strain rate response of sandwich composites. J Compos Struct 2000;50:279–85.
[5] Fatt MSH, Park KS. Dynamic models for low-velocity impact damage of composite sandwich panels—Part A: Deformation. J Compos Struct 2001;52:335–51.
[6] Fatt MSH, Park KS. Dynamic models for low-velocity impact damage of composite sandwich panels—Part B: Damage initiation. J Compos Struct 2001;52:353–64.
[7] Palazotto AN, Grummadi LNB, Vaidya UK, Herup EJ. Low velocity impact damage characteristics of Z-fiber reinforced sandwich panels-an experimental study. J Compos Struct 1999;43:275–88.
[8] Vaidya UK, Hosur MV, Earl D, Jeelani S. Impact response of integrated hollow core sandwich composite panels. J Compos Struct 2000;31:761–72.
[9] Asp LE, Nilsson KF. Delamination criticality in slender compression-loaded composite panels. J Eng Mater 2002;221–222:3–16.
[10] Kwon YW, Yoon SH, Sistare PJ. Compressive failure of carbon-foam sandwich composites with holes and/or partial delamination. J Compos Struct 1997;38:573–80.
[11] Carvelli V, DeAngelis D, Poggi C, Puoti R. Effects of manufacturing techniques on the mechanical properties of composite laminates. J Eng Mater 2002;221–222:109–20.
[12] Gustin J, Mahinfalah M, Nakhaie Jazar G, Rastgaar Aagaah M. Low velocity impact of sandwich composite plates. SEM Annual Conference and Exposition on Experimental and Applied Mechanics, North Carolina, June 2–4, 2003.
[13] Gustin J, Joneson A, Mahinfalah M, Stone J. Low velocity impact of combination Kevlar/carbon fiber sandwich composites. SEM International Congress and Exposition on Experimental and Applied Mechanics, Costa Mesa, CA, June 7–10, 2004.